


 Cite this: *Sens. Diagn.*, 2025, 4, 1103

## A near-infrared fluorescent aptanosensor enables selective detection of the stress hormone cortisol in artificial cerebrospinal fluid

 Jessica Kretli Zanetti,<sup>†a</sup> Maria Celina Stefoni,<sup>†ab</sup> Catarina Ferraz,<sup>a</sup> Amelia Ryan,<sup>a</sup> Atara Israel<sup>a</sup> and Ryan M. Williams \*<sup>ac</sup>

Cortisol is a hormone which regulates the body's response to stressors. Detection and monitoring of cortisol levels can provide information about physical and psychological health, thus it is essential to develop a sensor that can detect it in a sensitive manner. This study presents a biocompatible near-infrared fluorescent sensor, wherein single-walled carbon nanotubes (SWCNT) are functionalized with a cortisol-specific aptamer. We found this sensor was capable of detecting cortisol from 37.5  $\mu\text{g mL}^{-1}$  to 300  $\mu\text{g mL}^{-1}$  and that it was selective for cortisol compared to the similar molecule estrogen. Moreover, SWCNT functionalized with non-specific oligonucleotides did not exhibit a concentration-dependent response to cortisol, demonstrating the specificity provided by the aptamer sequence. The sensor also demonstrated the ability to detect cortisol in artificial cerebrospinal fluid. We anticipate that future optimization of this sensor will enable potential point-of-care or implantable device-based rapid detection of cortisol, with the potential for improving overall patient health and stress.

 Received 29th May 2025,  
 Accepted 18th September 2025

DOI: 10.1039/d5sd00085h

[rsc.li/sensors](https://rsc.li/sensors)

### Introduction

Cortisol is a steroid hormone that regulates essential physiological processes, including electrolyte balance, blood pressure, immune modulation, and metabolism.<sup>1</sup> The level of this hormone in biofluids varies throughout the day, reaching its peak in the morning and its lowest level at night.<sup>2</sup> Beyond its circadian rhythm, cortisol is secreted in response to stress, increasing blood pressure to provide metabolic energy from fat and glucose to muscles and brain. Prolonged exposure to stressors raises cortisol levels, thereby increasing the risk of cardiovascular diseases.<sup>3</sup> Moreover, elevated cortisol levels are associated with reduced cognitive functioning, higher risk of dementia, and development of Alzheimer's disease.<sup>4</sup> Thus, to support early diagnosis and intervention, it is imperative to monitor cortisol levels in a sensitive, specific, and cost-effective manner.

Several cortisol biosensors have been developed<sup>5–10</sup> using numerous detection methods, such as electrochemistry,<sup>11–21</sup> field-effects transistors (FETs),<sup>22,23</sup> FRET<sup>24</sup> and surface plasmon resonance (SPR).<sup>25</sup> For instance, cortisol detection was achieved in sweat using a wearable sensing device that includes a microfluidic chip and a three-electrode system, where the working electrode was modified with mesoporous silica nanochannels.<sup>26</sup> Another cortisol sensor developed<sup>27</sup> utilized competitive lateral flow immunoassay (LFIA) for cortisol detection in saliva, utilizing anti-cortisol antibodies that are functionalized both on gold nanoparticles and in the sensor's detection zone. Although these works successfully detected cortisol, they are not well-suited for implantable sensors. Optical sensors based on single-walled carbon nanotubes (SWCNT) offer a promising alternative.

Single-walled carbon nanotubes can be visualized as a single sheet of graphene rolled into a cylinder, denoted by an  $(n, m)$  index, determined by the vector along which this sheet is rolled.<sup>28</sup> SWCNT are inherently fluorescent in the tissue-transparent near infrared (NIR) region, and do not exhibit photobleaching, making them an ideal candidate for *in vitro* and *in vivo* applications.<sup>29,30</sup> SWCNT can be functionalized with biomolecular recognition elements or may have inherent binding to analytes of interest. The interaction of an analyte with the functionalized SWCNT surfaced modulates the fluorescence of the SWCNT, causing solvatochromic or intensity-based responses.<sup>29</sup> There have been several examples of DNA aptasensors incorporating SWCNT, wherein carbon

<sup>a</sup> Biomedical Engineering, The City College of New York, New York, NY 10031, USA.  
 E-mail: ryan.williams@stonybrookmedicine.edu

<sup>b</sup> Departamento de Química Inorgánica, Analítica y Química Física, Facultad de Ciencias Exactas y Naturales (DQIAQF), Universidad de Buenos Aires, and Instituto de Química Física de los Materiales, Medio Ambiente y Energía (INQUIMAE), CONICET-UBA, Buenos Aires C1428, Argentina

<sup>c</sup> Department of Medicine, Division of Nephrology & Hypertension, Stony Brook University, Stony Brook, NY 11794, USA

<sup>†</sup> Equal contribution.





### Sensor specificity assessments

To evaluate sensors specificity to cortisol, the biologically and chemically similar hormone  $\beta$ -estradiol (Fisher Scientific, Waltham, MA) was evaluated at an equal concentration to cortisol. Fluorescence was measured every 15 minutes over 3 hours and analyzed for shifts in center wavelength.

### Sensor performance on different media

To evaluate sensor performance in artificial sweat (a-sweat) and artificial cerebrospinal fluid (aCSF) (both from Fisher Scientific, Waltham, MA), a 100  $\mu$ L solution of 0.6 mg L<sup>-1</sup> of SWCNT-aptamer was added to each well, in both a-sweat and aCSF. Then, 20  $\mu$ L of 900  $\mu$ g mL<sup>-1</sup> of cortisol in 1% DMSO was added, yielding an 80% concentration of either a-sweat or aCSF in each well.

### Data analysis

All experiments were performed in triplicate. Samples which did not exhibit fluorescence, indicating poor or failed fluorescent detection, or non-physical (>20 nm) wavelength

changes, indicating poor measurement or fit, were excluded. Individual SWCNT chiral emission peaks were identified according to published studies.<sup>41,45</sup> Each peak was fit using a pseudo-Voigt model with a custom MATLAB code (code available upon request) and data were used for analyses when model fit  $R^2$  was greater than 0.95. Triplicate averages and mean standard deviations were obtained and reported. Intensity changes and center wavelength shifts were normalized by subtracting the sample response to SWCNT intensity/center wavelength in 1% DMSO in absence of any analyte. One-way ANOVA analysis was performed with Tukey posthoc analyses.

## Results and discussion

### The aptanosensor demonstrates sensitive concentration-dependent response to cortisol

In order to engineer a fluorescent aptanosensor for the stress hormone cortisol, we non-covalently suspended the SWCNT in solution directly with a cortisol-selective aptamer (Fig. 1A). HiPCO SWCNTs were suspended well in solution with each of

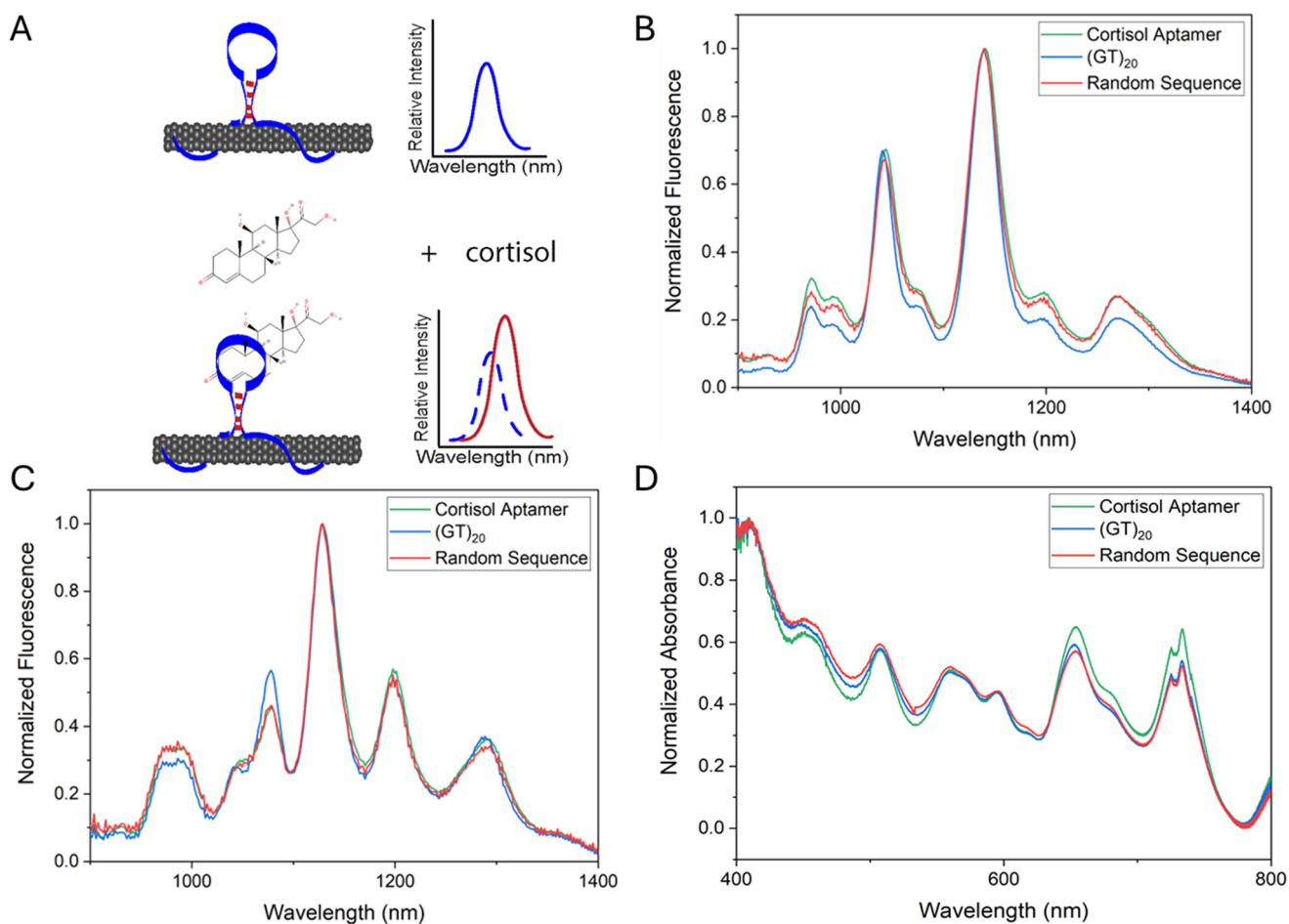


**Fig. 1** Cortisol detection strategy and sensor/control characterization. A) A SWCNT-based aptanosensor detection strategy for the stress hormone cortisol. Fluorescence spectra of SWCNT functionalized with cortisol aptamer, (GT)<sub>20</sub> and a random 40mer sequence with laser excitation at (B) 655 nm and (C) 730 nm. (D) UV-vis absorbance spectra of the SWCNT constructs.



the cortisol aptamer, (GT)<sub>20</sub> ssDNA, and random 40-mer ssDNA sequence. The resulting constructs were inherently fluorescent under red laser (655 nm and 730 nm) excitation (Fig. 1B and C). The UV-vis spectra of these (Fig. 1D) demonstrate that each of the 3 sequence-SWCNT constructs were suspended well in solution with multiple abundant SWCNT species present.

When dispersed with ssDNA, SWCNT are typically water soluble. However, cortisol is not water soluble, and thus it was necessary to select a solvent to solubilize cortisol while minimizing interference with the SWCNT fluorescence. To evaluate the influence of the solvent on sensors fluorescence, ethanol, 1% DMSO, and 0.1% DMSO, were added to the SWCNT-aptamer construct. The addition of 0.1% DMSO and 1% DMSO caused a center wavelength shift (Fig. S1A) comparable to the addition of PBS. However, SWCNT

fluorescence in 0.1% DMSO behaved differently over time than PBS, exhibiting more pronounced center wavelength shifts (Fig. S1C). When analyzing the (7,6) peak, the behavior observed with 1% DMSO was also the most similar to that in PBS (Fig. S2). Therefore, we performed all further sensor analysis in 1% DMSO.

We then evaluated sensor response to increasing cortisol concentrations from 37.5  $\mu\text{g mL}^{-1}$  to 300  $\mu\text{g mL}^{-1}$ . The concentration response was analyzed with (6,5)-enriched carbon nanotubes (Fig. S3). The (7,5) and (7,6) peaks exhibited a positive correlation between wavelength change and concentration, though neither did for intensity. The only significant difference to the absence of cortisol was obtained at 125  $\mu\text{g mL}^{-1}$ , hence, a concentration range was evaluated around this value with HiPCO SWCNTs. With aptamer functionalized HiPCO SWCNTs, the

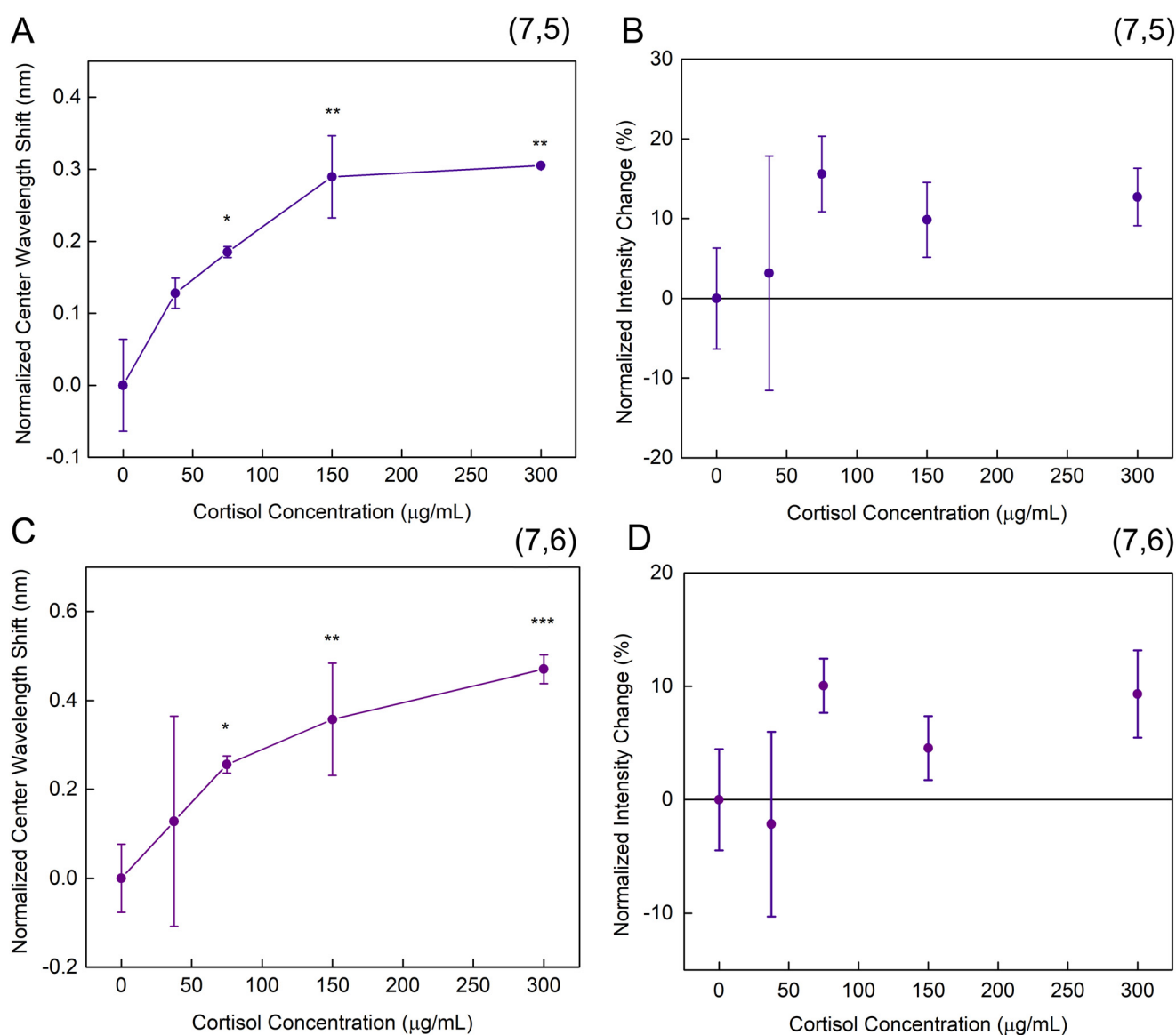


Fig. 2 Dynamic range of aptanosensor response to cortisol. (A) Normalized center wavelength shift and (B) normalized intensity change, in (7,5) SWCNTs peak with increasing cortisol concentration after 3 hours. (C) Normalized center wavelength shift and (D) normalized intensity change, in (7,6) SWCNTs peak with increasing cortisol concentration after 3 hours. \* =  $p < 0.5$ , \*\* =  $p < 0.01$ , \*\*\* =  $p < 0.001$ .



center wavelength shift of (7,5) and (7,6) peaks increased with higher cortisol concentrations, reaching a plateau around 300  $\mu\text{g mL}^{-1}$  (Fig. 2A and C). Although both chiralities exhibit a monotonic response to cortisol and reach the plateau around the same concentration, the concentration curves are different. This could be attributed to the unique conformational structures that each SWCNT lattice induce in the aptamer, therefore, both chiralities were analyzed.<sup>46–48</sup> Though shifts as small as 0.2–0.3 nm were observed, they were repeatable, with a small variability that significantly differed from controls. This response appeared to be concentration-dependent and consistent with a site-specific binding curve that saturated at higher concentrations. The intensity changes appeared to be somewhat binary (Fig. 2B and D), with detection was noted between 75–300  $\mu\text{g mL}^{-1}$ . The aptamer-SWCNT sensor presented in this work exhibited detection of cortisol from 37.5  $\mu\text{g mL}^{-1}$  to 300  $\mu\text{g mL}^{-1}$ . As 37.5  $\mu\text{g mL}^{-1}$  was the lowest concentration we evaluated, it did not approach the clinically relevant range in sweat from 0.008–0.141  $\mu\text{g mL}^{-1}$ .<sup>49</sup> However, this is within the range of the prior study which performed CoPhMoRe-based SWCNT sensor development, as the cortisol sensor in that work operated linearly between  $\sim 10$ –70  $\mu\text{g mL}^{-1}$ .<sup>39</sup> Potential improvements in the detection range could be attained by using chirality-sorted SWCNTs to limit spectral overlap<sup>50–52</sup> and by exploring other cortisol aptamers.<sup>53–55</sup>

#### The aptanosensor induces specific response to cortisol while non-specific ssDNA sequences do not

In this work, we developed a fluorescence nanosensor for cortisol using an aptameric biorecognition element. To evaluate whether other unspecific DNA sequences could also interact with cortisol, the response of SWCNT-(GT)<sub>20</sub> and SWCNT-random 40mer sequence was evaluated. The (7,5) peak of SWCNT-(GT)<sub>20</sub> (Fig. 3A) exhibited a minimal blue-shift consistent with linear non-specific adsorption. The SWCNT-random 40mer sequence construct also demonstrated very minor wavelength shifts in the (7,5) peak, with no clear correlation with cortisol concentration. For the (7,6) peak, both the SWCNT-(GT)<sub>20</sub> and the SWCNT-random 40mer sequence constructs demonstrated a relatively minor concentration-dependent response (Fig. 3C), again consistent with linear non-specific adsorption to the surface of the nanotube most likely. The center wavelength shift response of these three constructs over the three hour period was also evaluated (Fig. S4 and S5), all exhibiting a sharp shift in the first 15 minutes. Neither control sequence demonstrated a significant intensity change at either chirality observed (Fig. 3B and D). A minor increase in intensity is observed for both chiralities with (GT)<sub>20</sub>, also likely consistent with non-specific adsorption to the surface of the carbon nanotube.

#### The aptanosensor selectively detects cortisol and not estradiol

The selectivity of the sensor towards cortisol was evaluated by comparing the construct's response to estradiol. Estradiol, a

form of estrogen, has structural similarities to cortisol (Fig. 4A and B) and both hormones are found in similar bodily fluids.<sup>56</sup>

The selectivity of center wavelength shifts for the (7,5) peak was statistically significant for cortisol compared to estrogen at the low and high tested concentrations, likely due to variability in the 150  $\mu\text{g mL}^{-1}$  measurement (Fig. 4C), while the intensity change was selective only at 300  $\mu\text{g mL}^{-1}$  (Fig. 4D). For the (7,6) peak, the center wavelength shift was selective at low and high concentrations, again due to variability in the middle test value (Fig. 4E). The intensity change, however, was significantly at all three concentrations tested (Fig. 4F). Notably, sensor center wavelength shifts in response to estradiol were in the same direction as cortisol, though slightly less. In contrast, the changes in intensity have a distinct opposite response for each hormone, which is more pronounced at higher concentrations. In comparison, the previous CoPhMoRe-SWCNT approach to cortisol detection found that the intensity-based response to estradiol was  $\sim 50\%$  of that compared to cortisol at  $\sim 37 \mu\text{g mL}^{-1}$  of analyte.<sup>39</sup> Potential improvements in selectivity of wavelength response may be made by screening passivation agents to coat the SWCNT surface to block any nonspecific interactions.<sup>57</sup> This is further strengthened by prior molecular dynamics simulations with cortisol and the CoPhMoRe-SWCNT sensor, demonstrating cortisol may interact with the SWCNT surface within a polymeric binding pocket, thus indicating the necessity of directing interactions to the sensing element in the current design.<sup>39</sup>

#### Sensor performance in aCSF and a-sweat

To further evaluate the translational potential of this sensor, it was evaluated in 80% artificial sweat (a-sweat) and artificial cerebrospinal fluid (aCSF), which represent two potential complex biofluids in which elevated cortisol levels may be found in disease conditions. For example, cortisol levels are elevated in the CSF of patients with acute bacterial meningitis as well as cognitive impairment, which directly correlated with increased levels of inflammatory cytokines such as IL-6, TNF- $\alpha$ , and IL-1 $\beta$ , whereas decreased levels of cortisol are found in the CSF of patients with multiple sclerosis.<sup>58–60</sup> Cortisol levels in the sweat are also directly linked to systemic stress levels.<sup>61</sup> We found the aptanosensor demonstrated a significant wavelength and intensity change to 150  $\mu\text{g mL}^{-1}$  cortisol in aCSF (Fig. 5). Neither peak, however, demonstrated a significant response to 150  $\mu\text{g mL}^{-1}$  of cortisol in artificial sweat, potentially due to pH-induced aptamer conformational changes in sweat.<sup>62</sup> While the previous cortisol SWCNT sensor was not tested in these biofluids, nor *in vivo*, the related progesterone sensor from the same study was embedded in a hydrogel and implanted into mice,<sup>30</sup> wherein it was able to report the presence of progesterone.<sup>39</sup>



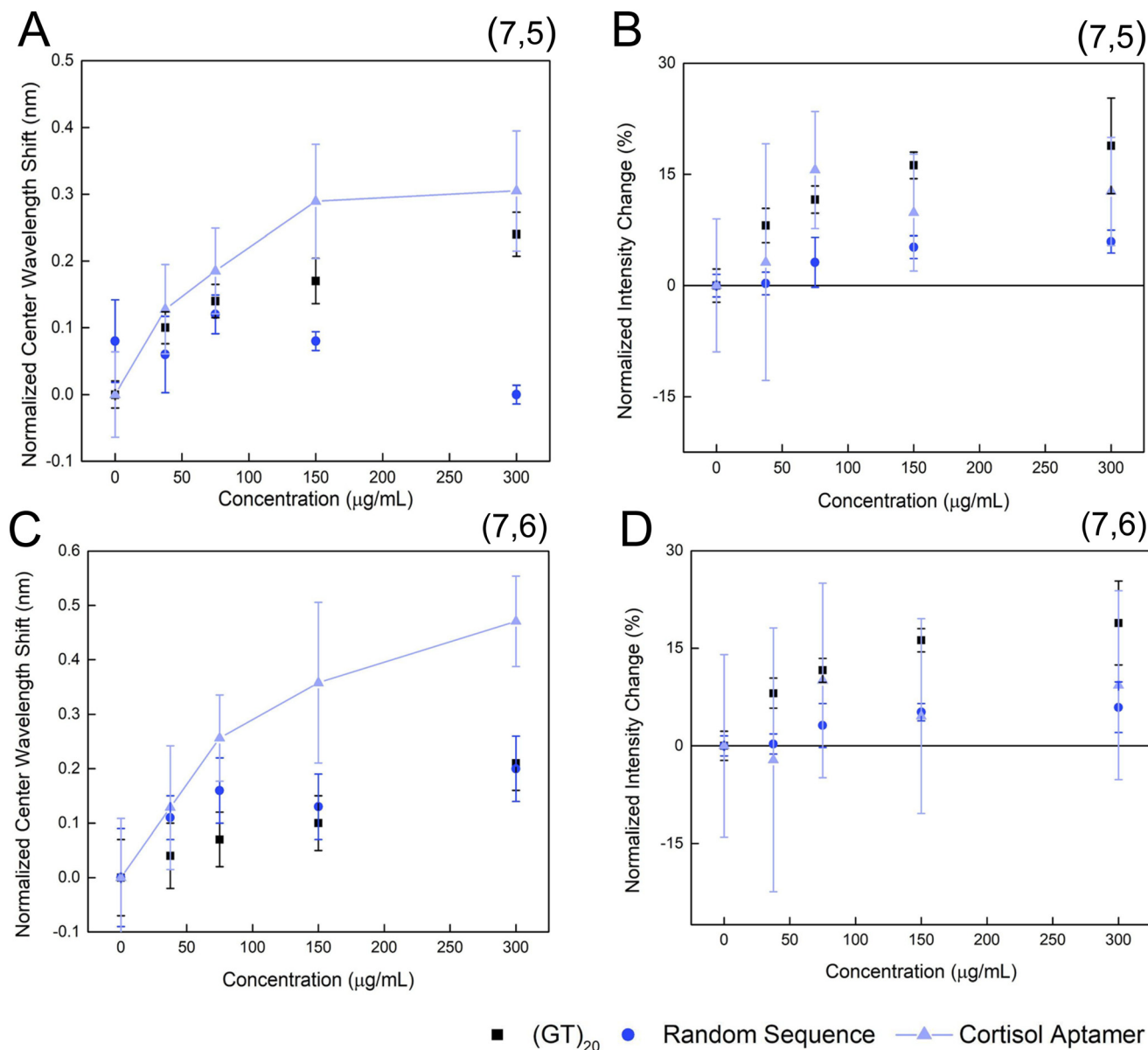


**Fig. 3** The cortisol aptamer induces a concentration-dependent response while non-specific ssDNA sequences do not. (A) Normalized center wavelength shift and (B) normalized intensity change, for the (7,5) chirality of HiPCO SWCNT functionalized with (GT)<sub>20</sub>, a cortisol-specific aptamer, and a 40-mer random sequence constructs. (C) Normalized center wavelength shift and (D) normalized intensity change, for the (7,6) HiPCO SWCNT functionalized with (GT)<sub>20</sub>, a cortisol-specific aptamer, and a 40-mer random sequence.

The biorecognition capabilities of an aptamer can be influenced by pH, either through protonation of the binding site or by partial denaturation of the aptamer structure, which may impact sensor performance in sweat samples.<sup>63</sup> It is well-established that aptamer functionality is closely-related to the conditions in which it was selected, especially pH and salt concentrations,<sup>64,65</sup> and thus it may be necessary to buffer pH if this aptamer is used, or to use a different aptamer sequence tailored to each condition. For pending clinical translation, it would be necessary to evaluate the stability of the aptamer, sensor construct, and signal in various buffers and over time.

## Conclusions

In this work, we engineered a SWCNT-aptamer based sensor for the stress hormone cortisol. The sensor demonstrated a center wavelength shift and intensity change in the presence of cortisol, whereas non-specific ssDNA sequences complexed with SWCNT did not. The sensor also demonstrated selective changes in intensity for cortisol compared to the similar molecule estradiol. Moreover, the sensor exhibited response to cortisol in aCSF, showing its potential use for clinical applications. Overall, the findings indicate that our engineered cortisol aptananosensor holds promise as a potential diagnostic tool. Compared to traditional methods,



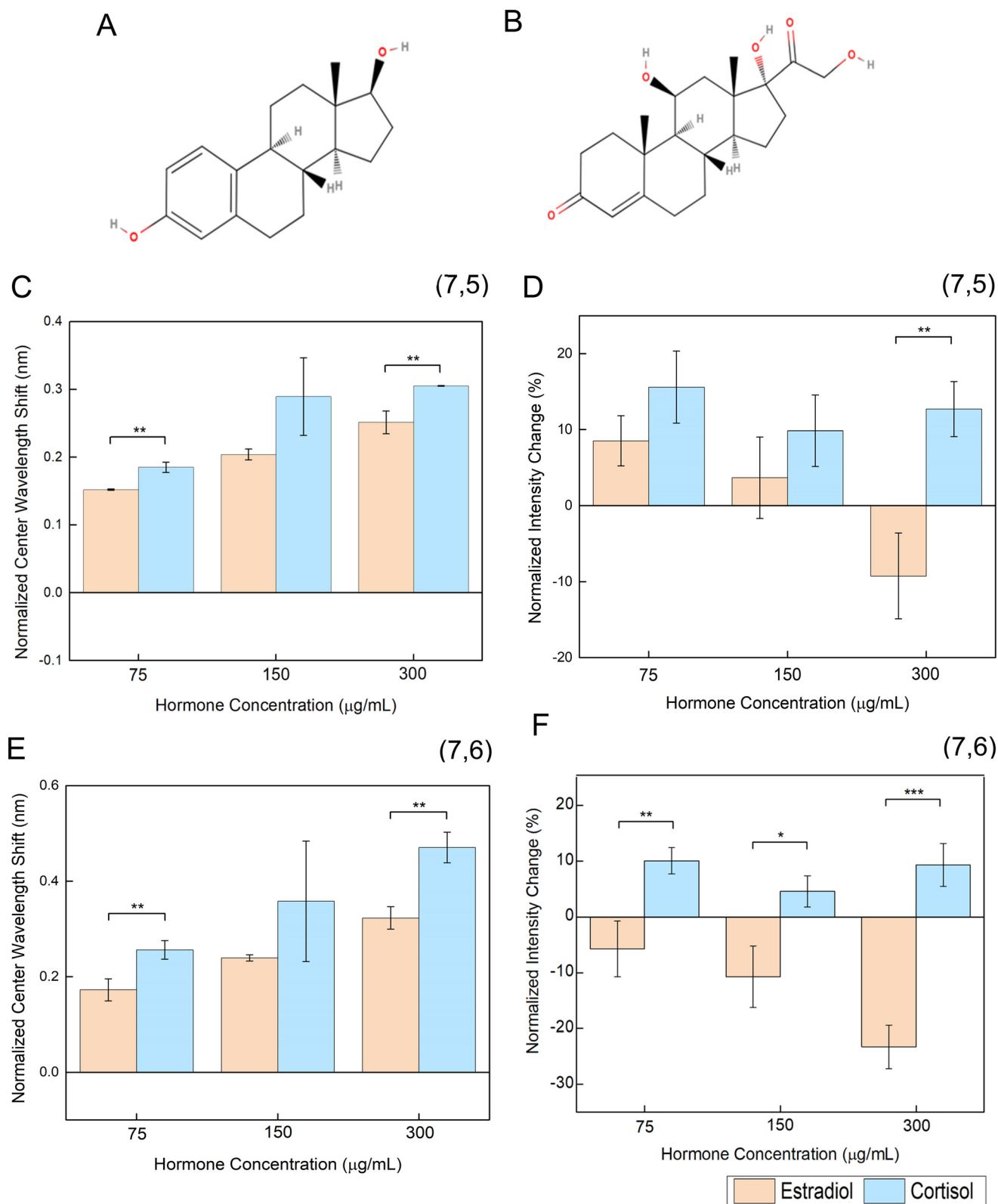


**Fig. 4** The aptanosensor selectively detects cortisol and not estrogen. Structures of (A) cortisol and (B) estradiol. (C) Normalized center wavelength shift and (D) intensity change for the (7,5) peak of HiPCO SWCNT-aptamer sensor. (E) Normalized center wavelength shift and (F) intensity change, for the (7,6) peak of HiPCO SWCNT-aptamer sensor. \* =  $p < 0.05$ , \*\* =  $p < 0.01$ ; \*\*\* =  $p < 0.001$ .



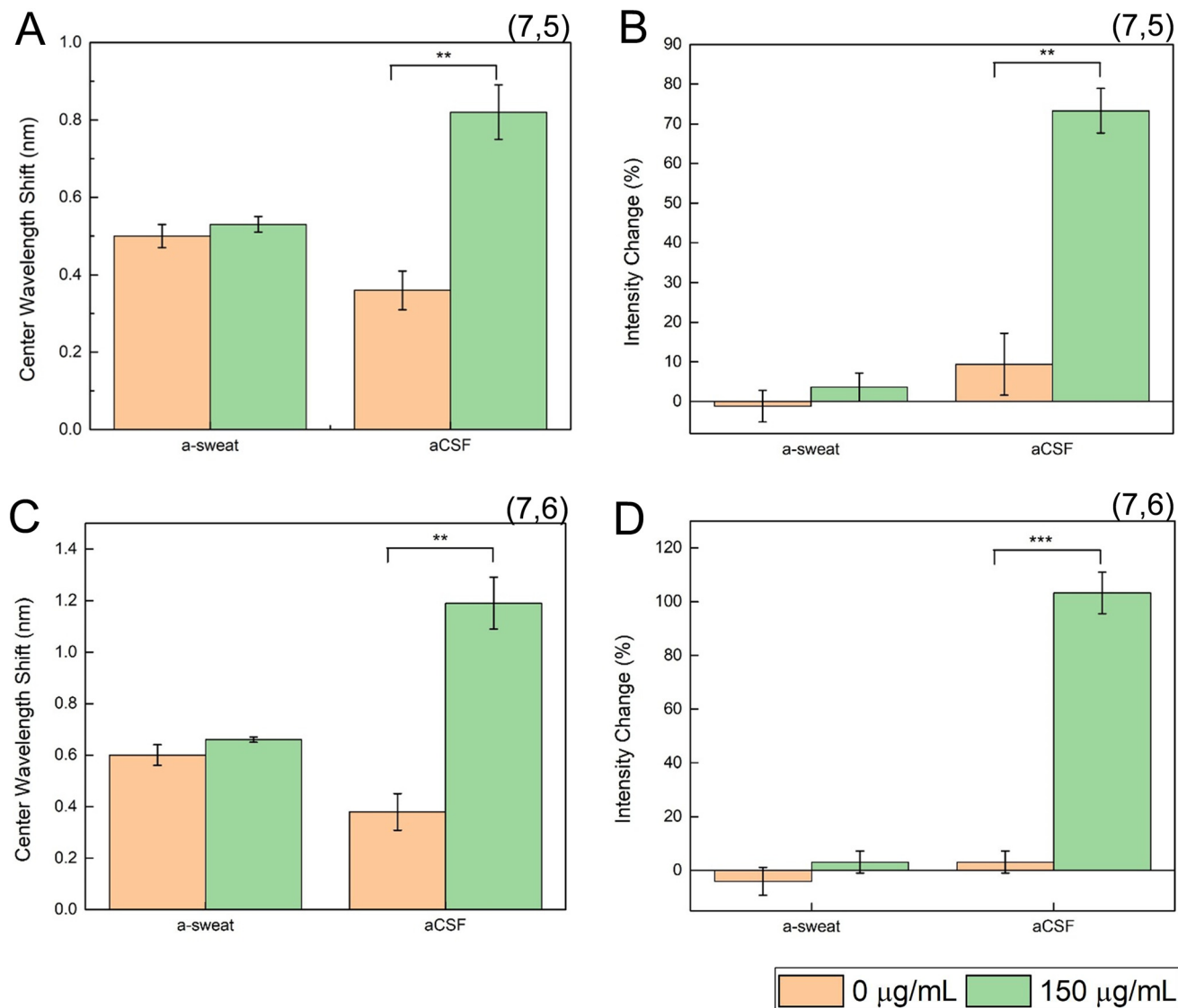


Fig. 5 The aptanosensor is capable of detecting cortisol in aCSF. Center wavelength shift (A) and intensity change (B) for the (7,5) peak of HiPCO SWCNT-aptamer sensor, in a-sweat and aCSF. Center wavelength shift (C) and intensity change (D) for the (7,6) peak of HiPCO SWCNT-aptamer sensor, in a-sweat and aCSF. \*\* =  $p < 0.01$ , \*\*\* =  $p < 0.001$ .

this approach offers the potential for *in vivo* monitoring and point-of-care detection, in a cost-effective cortisol manner.

## Conflicts of interest

There are no conflicts of interest to declare.

## Data availability

Supplementary information is available. See DOI: <https://doi.org/10.1039/D5SD00085H>.

Raw and processed spectral data will be made available to requesters upon reasonable request. Matlab code used for data processing will also be made available to requesters upon reasonable request.

## Acknowledgements

The authors wish to acknowledge all members of the Williams Lab for discussion and feedback. This work was supported by NIH R35GM142833 (R. Williams) and the support of The City College of New York Grove School of Engineering. A. Ryan and A. Israel were supported by a G-RISE Ph.D. traineeship from the National Institutes of Health (T32GM136499).

## References

- 1 L. Thau, J. Gandhi and S. Sharma, *Physiology, Cortisol*, StatPearls Publishing, 2023.
- 2 S. Sakihara, K. Kageyama, Y. Oki, M. Doi, Y. Iwasaki, S. Takayasu, T. Moriyama, K. Terui, T. Nigawara, Y. Hirata, K. Hashimoto and T. Suda, Evaluation of plasma, salivary, and



- urinary cortisol levels for diagnosis of Cushing's syndrome, *Endocr. J.*, 2010, **57**(4), 331–337, DOI: [10.1507/endocrj.k09e-340](https://doi.org/10.1507/endocrj.k09e-340).
- 3 J. A. Whitworth, P. M. Williamson, G. Mangos and J. J. Kelly, Cardiovascular consequences of cortisol excess, *Vasc. Health Risk Manage.*, 2005, **1**(4), 291–299.
  - 4 S. Ouanes and J. Popp, High Cortisol and the Risk of Dementia and Alzheimer's Disease: A Review of the Literature, *Front. Aging Neurosci.*, 2019, **11**, 43, DOI: [10.3389/fnagi.2019.00043](https://doi.org/10.3389/fnagi.2019.00043).
  - 5 R. Santonocito, R. Puglisi, A. Cavallaro, A. Pappalardo and G. T. Sfrazzetto, Cortisol sensing by optical sensors, *Analyst*, 2023, **149**(4), 989–1001, DOI: [10.1039/D3AN01801F](https://doi.org/10.1039/D3AN01801F).
  - 6 J. Ok, S. Park, Y. H. Jung and T. Kim, Wearable and Implantable Cortisol-Sensing Electronics for Stress Monitoring, *Adv. Mater.*, 2023, **36**, 2211595, DOI: [10.1002/adma.202211595](https://doi.org/10.1002/adma.202211595).
  - 7 G. E. Yilmaz, Y. Saylan and A. Denizli, A review for cortisol sensing in medical applications, *J. Pharm. Biomed. Anal.*, 2024, **4**, 100045, DOI: [10.1016/j.jpba.2024.100045](https://doi.org/10.1016/j.jpba.2024.100045).
  - 8 U. A. Wankhade, Y. Thakare, B. M. Hardas and R. S. Pande, Cortisol Detection Methods for Stress Monitoring: Current Insight and Future Prospect: A Review, *IEEE Sens. J.*, 2024, **24**(15), 23389–23400, DOI: [10.1109/JSEN.2024.3404399](https://doi.org/10.1109/JSEN.2024.3404399).
  - 9 F. Gao, C. Liu, L. Zhang, T. Liu, Z. Wang, Z. Song, H. Cai, Z. Fang, J. Chen, J. Wang, M. Han, J. Wang, K. Lin, R. Wang, M. Li, Q. Mei, X. Ma, S. Liang, G. Gou and N. Xue, Wearable and flexible electrochemical sensors for sweat analysis: a review, *Microsyst. Nanoeng.*, 2023, **9**, 1, DOI: [10.1038/s41378-022-00443-6](https://doi.org/10.1038/s41378-022-00443-6).
  - 10 V. Vignesh, B. Castro-Dominguez, T. D. James, J. M. Gamble-Turner, S. Lightman and N. M. Reis, Advancements in Cortisol Detection: From Conventional Methods to Next-Generation Technologies for Enhanced Hormone Monitoring, *ACS Sens.*, 2024, **9**(4), 1666–1681, DOI: [10.1021/acssensors.3c01912](https://doi.org/10.1021/acssensors.3c01912).
  - 11 C. J. Weber, O. M. Clay, R. E. Lycan, G. K. Anderson and O. Simoska, Advances in electrochemical biosensor design for the detection of the stress biomarker cortisol, *Anal. Bioanal. Chem.*, 2023, **416**(1), 87–106, DOI: [10.1007/s00216-023-05047-1](https://doi.org/10.1007/s00216-023-05047-1).
  - 12 Q. Liu, W. Shi, L. Tian, M. Su, M. Jiang, J. Li, H. Gu and C. Yu, Preparation of nanostructured PDMS film as flexible immunosensor for cortisol analysis in human sweat, *Anal. Chim. Acta*, 2021, **1184**, 339010, DOI: [10.1016/j.aca.2021.339010](https://doi.org/10.1016/j.aca.2021.339010).
  - 13 L. Fiore, V. Mazzaracchio, A. Serani, G. Fabiani, L. Fabiani, G. Volpe, D. Moscone, G. M. Bianco, C. Occhiuzzi, G. Marrocco and F. Arduini, Microfluidic paper-based wearable electrochemical biosensor for reliable cortisol detection in sweat, *Sens. Actuators, B*, 2023, **379**, 133258, DOI: [10.1016/j.snb.2022.133258](https://doi.org/10.1016/j.snb.2022.133258).
  - 14 N. K. Singh, S. Chung, M. Sveiven and D. A. Hall, Cortisol Detection in Undiluted Human Serum Using a Sensitive Electrochemical Structure-Switching Aptamer over an Antifouling Nanocomposite Layer, *ACS Omega*, 2021, **6**(42), 27888–27897, DOI: [10.1021/acsomega.1c03552](https://doi.org/10.1021/acsomega.1c03552).
  - 15 A. R. Naik, Y. Zhou, A. A. Dey, D. L. G. Arellano, U. Okoroanyanwu, E. B. Secor, M. C. Hersam, J. Morse, J. P. Rothstein, K. R. Carter and J. J. Watkins, Printed microfluidic sweat sensing platform for cortisol and glucose detection, *Lab Chip*, 2022, **22**, 156–169, DOI: [10.1039/d1lc00633a](https://doi.org/10.1039/d1lc00633a).
  - 16 S. Yeasmin, B. Wu, Y. Liu, A. Ullah and L.-J. Cheng, Nano gold-doped molecularly imprinted electrochemical sensor for rapid and ultrasensitive cortisol detection, *Biosens. Bioelectron.*, 2022, **206**, 114142, DOI: [10.1016/j.bios.2022.114142](https://doi.org/10.1016/j.bios.2022.114142).
  - 17 X. Xu, P. Clément, J. Eklöf-Österberg, N. Kelley-Loughnane, K. Moth-Poulsen, J. L. Chávez and M. Palma, Reconfigurable Carbon Nanotube Multiplexed Sensing Devices, *Nano Lett.*, 2018, **18**(7), 4130–4135, DOI: [10.1021/acs.nanolett.8b00856](https://doi.org/10.1021/acs.nanolett.8b00856).
  - 18 Z. Huang, H. Chen, Y. Huarong, Z. Chen, N. Jaffrezic-Renault and Z. Guo, An ultrasensitive aptamer-antibody sandwich cortisol sensor for the noninvasive monitoring of stress state, *Biosens. Bioelectron.*, 2021, **190**, 113451, DOI: [10.1016/j.bios.2021.113451](https://doi.org/10.1016/j.bios.2021.113451).
  - 19 P. Karthika, S. Shanmuganathan, V. Subramanian and C. Delerue-Matos, Selective detection of salivary cortisol using screen-printed electrode coated with molecularly imprinted polymer, *Talanta*, 2024, **272**, 125923, DOI: [10.1016/j.talanta.2024.125823](https://doi.org/10.1016/j.talanta.2024.125823).
  - 20 A. Sharma, A. Wulff, A. Thomas and S. Sonkusale, Ultrasensitive electrochemical sensor for detection of salivary cortisol in stress conditions, *Microchim. Acta*, 2024, **191**(2), 103, DOI: [10.1007/s00604-023-06169-0](https://doi.org/10.1007/s00604-023-06169-0).
  - 21 N. K. Singh, S. Chung, A.-Y. Chang, J. Wang and D. A. Hall, A non-invasive wearable stress patch for real-time cortisol monitoring using a pseudoknot-assisted aptamer, *Biosens. Bioelectron.*, 2023, **227**, 115097, DOI: [10.1016/j.bios.2023.115097](https://doi.org/10.1016/j.bios.2023.115097).
  - 22 L. Bian, W. Shao, Z. Liu, Z. Zeng and A. Star, Detection of Stress Hormone with Semiconducting Single-Walled Carbon Nanotube-Based Field-Effect Transistors, *J. Electrochem. Soc.*, 2022, **169**, 057519, DOI: [10.1149/1945-7111/ac6e8d](https://doi.org/10.1149/1945-7111/ac6e8d).
  - 23 S. Sheibani, L. Capua, S. Kamaei, S. S. A. Akbari, J. Zhang, H. Guerin and A. M. Ionescu, Extended gate field-effect-transistor for sensing cortisol stress hormone, *Commun. Mater.*, 2021, **2**, 10, DOI: [10.1038/s43246-020-00114-x](https://doi.org/10.1038/s43246-020-00114-x).
  - 24 X. Weng, Z. Fu, C. Zhang, W. Jiang and H. Jiang, A Portable 3D Microfluidic Origami Biosensor for Cortisol Detection in Human Sweat, *Anal. Chem.*, 2022, **94**(8), 3526–3534, DOI: [10.1021/acs.analchem.1c04508](https://doi.org/10.1021/acs.analchem.1c04508).
  - 25 C. Blackburn, M. V. Sullivan, M. I. Wild, A. J. O'Connor and N. W. Turner, Utilisation of molecularly imprinting technology for the detection of glucocorticoids for a point of care surface plasmon resonance (SPR) device, *Anal. Chim. Acta*, 2024, **1285**, 342004, DOI: [10.1016/j.aca.2023.342004](https://doi.org/10.1016/j.aca.2023.342004).
  - 26 Y. Luan, Y. Zhou, C. Li, H. Wang, Y. Zhou, Q. Wang, X. He, J. Huang, J. Liu, X. Yang and K. Wang, Wearable Sensing Device Integrated with Prestored Reagents for Cortisol Detection in SweatClick, *ACS Sens.*, 2024, **9**(4), 2075–2082, DOI: [10.1021/acssensors.4c00112](https://doi.org/10.1021/acssensors.4c00112).
  - 27 S. Kim and M.-G. Kim, Automatically Signal-Enhanced Lateral Flow Immunoassay for Ultrasensitive Salivary Cortisol Detection, *Anal. Chem.*, 2025, **97**(5), 2707–2713, DOI: [10.1021/acs.analchem.4c04700](https://doi.org/10.1021/acs.analchem.4c04700).



- 28 M. J. O'Connell, M. B. Sergei, C. B. Huffman, V. C. Moore, M. S. Strano, E. H. Haroz, K. L. Rialon, P. J. Boul, W. H. Noon, C. Kittrell, J. Ma, R. H. Hauge, R. B. Weisman and R. E. Smalley, Band gap fluorescence from individual single-walled carbon nanotubes, *Science*, 2002, **297**(5581), 593–596.
- 29 Z. Cohen and R. M. Williams, Single-Walled Carbon Nanotubes as Optical Transducers for Nanobiosensors In VivoClick to copy article link, *ACS Nano*, 2024, **18**(52), 35164–35181, DOI: [10.1021/acsnano.4c13076](https://doi.org/10.1021/acsnano.4c13076).
- 30 Z. Cohen and R. M. Williams, Single-walled carbon nanotubes as optical transducers for nanobiosensors in vivo, *ACS Nano*, 2024, **18**(52), 35164–35181.
- 31 K. Lee, N. Amirali, J. Jeon, C. Y. Lee and K. Yum, Near-Infrared Fluorescence Modulation of Refolded DNA Aptamer-Functionalized Single-Walled Carbon Nanotubes for Optical Sensing, *ACS Appl. Nano Mater.*, 2018, **1**(9), 5327–5336.
- 32 X. W. Guo, F. Wen, N. Zheng, M. Saive, M.-L. Fauconnier and J. Wang, Aptamer-based biosensor for detection of mycotoxins, *Front. Chem.*, 2020, **8**, 195.
- 33 A. K. Ryan, S. Rahman and R. M. Williams, Optical Aptamer-Based Cytokine Nanosensor Detects Macrophage Activation by Bacterial Toxins, *ACS Sens.*, 2024, **9**(7), 3697–3706, DOI: [10.1021/acssensors.4c00887](https://doi.org/10.1021/acssensors.4c00887).
- 34 M. N. Dinarvand, E. Neubert, D. Meyer, G. Selvaggio, F. A. Mann, L. Erpenbeck and S. Kruss, Near-Infrared Imaging of Serotonin Release from Cells with Fluorescent Nanosensors, *Nano Lett.*, 2019, **19**(9), 6604–6611.
- 35 H. Wu, R. Nifšler, V. Morris, N. Herrmann, P. Hu, S.-J. Jeon, S. Kruss and J. P. Giraldo, Monitoring Plant Health with Near-Infrared Fluorescent H<sub>2</sub>O<sub>2</sub> Nanosensors, *Nano Lett.*, 2020, **20**(4), 2432–2442.
- 36 R. Nifšler, L. Kurth, H. Li, A. Spreinat, I. Kuhlemann, B. S. Flavel and S. Kruss, Sensing with Chirality-Pure Near-Infrared Fluorescent Carbon Nanotubes, *Anal. Chem.*, 2021, **93**(16), 6446–6455.
- 37 R. Ehrlich, A. Hendler-Neumark, V. Wulf, D. Amir and G. Bisker, Optical Nanosensors for Real-Time Feedback on Insulin Secretion by  $\beta$ -Cells, *Small*, 2021, **17**(30), 2101660.
- 38 M. P. Landry, H. Ando, A. Y. Chen, J. Cao, V. I. Kottadiel, L. Chio, D. Yang, J. Dong, T. K. Lu and M. S. Strano, Single-molecule detection of protein efflux from microorganisms using fluorescent single-walled carbon nanotube sensor arrays, *Nat. Nanotechnol.*, 2017, **12**(4), 368–377.
- 39 M. A. Lee, S. Wang, X. Jin, N. A. Bakh, F. T. Nguyen, J. Dong, K. S. Silmore, X. Gong, C. Pham, K. K. Jones, S. Muthupalani, G. Bisker, M. Son and M. S. Strano, Implantable Nanosensors for Human Steroid Hormone Sensing In Vivo Using a Self-Templating Corona Phase Molecular Recognition, *Adv. Healthcare Mater.*, 2020, **9**(21), e2000429, DOI: [10.1002/adhm.202000429](https://doi.org/10.1002/adhm.202000429).
- 40 J. A. Martin, J. L. Chávez, Y. Chushak, R. R. Chapleau, J. Hagen and N. Kelley-Loughnane, Tunable stringency aptamer selection and gold nanoparticle assay for detection of cortisol, *Anal. Bioanal. Chem.*, 2014, **406**(19), 4637–4647, DOI: [10.1007/s00216-014-7883-8](https://doi.org/10.1007/s00216-014-7883-8).
- 41 M. Zheng, A. Jagota, E. D. Semke, B. A. Diner, R. S. McLean, S. R. Lustig, R. E. Richardson and N. G. Tassi, DNA-assisted dispersion and separation of carbon nanotubes, *Nat. Mater.*, 2003, **2**(5), 338–342, DOI: [10.1038/nmat877](https://doi.org/10.1038/nmat877).
- 42 S. Dalirirad and A. J. Steckl, Aptamer-based lateral flow assay for point of care cortisol detection in sweat, *Sens. Actuators, B*, 2019, **283**, 79–86, DOI: [10.1016/j.snb.2018.11.161](https://doi.org/10.1016/j.snb.2018.11.161).
- 43 K. Lei, S. M. Bachilo and R. B. Weisman, Kinetics of Single-Wall Carbon Nanotube Coating Displacement by Single-Stranded DNA Depends on Nanotube Structure, *ACS Nano*, 2023, **17**(17), 17568–17575, DOI: [10.1021/acsnano.3c06906](https://doi.org/10.1021/acsnano.3c06906).
- 44 R. Nifšler, F. A. Mann, P. Chaturvedi, J. Horlebein, D. Meyer, L. Vuković and S. Kruss, Quantification of the Number of Adsorbed DNA Molecules on Single-Walled Carbon Nanotubes, *J. Phys. Chem. C*, 2019, **123**(8), 4837–4847, DOI: [10.1021/acs.jpcc.8b11058](https://doi.org/10.1021/acs.jpcc.8b11058).
- 45 A. K. Ryan, S. Rahman and R. M. Williams, Optical Aptamer-Based Cytokine Nanosensor Detects Macrophage Activation by Bacterial Toxins, *ACS Sens.*, 2024, **9**(7), 3697–3706, DOI: [10.1021/acssensors.4c00887](https://doi.org/10.1021/acssensors.4c00887).
- 46 M. P. Landry, L. Vukovic, S. Kruss, G. Bisker, A. M. Landry, S. Islam, R. Jain, K. Schulten and M. S. Strano, Comparative Dynamics and Sequence Dependence of DNA and RNA Binding to Single Walled Carbon Nanotubes, *J. Phys. Chem. C Nanomater Interfaces*, 2015, **119**(18), 10048–10058, DOI: [10.1021/jp511448e](https://doi.org/10.1021/jp511448e).
- 47 Z. Li, Y. Song, A. Li, W. Xu and W. Zhang, Direct observation of the wrapping/unwrapping of ssDNA around/from a SWCNT at the single-molecule level: towards tuning the binding mode and strength, *Nanoscale*, 2018, **10**(39), 18586–18596, DOI: [10.1039/c8nr06150e](https://doi.org/10.1039/c8nr06150e).
- 48 D. Roxbury, J. Mittal and A. Jagota, Molecular-basis of single-walled carbon nanotube recognition by single-stranded DNA, *Nano Lett.*, 2012, **12**(3), 1464–1469, DOI: [10.1021/nl204182b](https://doi.org/10.1021/nl204182b).
- 49 E. Russell, G. Koren, M. Rieder and S. H. M. Van Uum, The detection of cortisol in human sweat: implications for measurement of cortisol in hair, *Ther. Drug Monit.*, 2014, **36**(1), 30–34, DOI: [10.1097/FTD.0b013e31829daa0a](https://doi.org/10.1097/FTD.0b013e31829daa0a).
- 50 R. Nifšler, J. Ackermann, C. Ma and S. Kruss, Prospects of Fluorescent Single-Chirality Carbon Nanotube-Based Biosensors, *Anal. Chem.*, 2022, **94**(28), 9941–9951, DOI: [10.1021/acs.analchem.2c01321](https://doi.org/10.1021/acs.analchem.2c01321).
- 51 F. Yang, M. Wan, D. Zhang, J. Yang, M. Zheng and Y. Li, Chirality Pure Carbon Nanotubes: Growth, Sorting, and Characterization, *Chem. Rev.*, 2020, **120**(5), 2693–2758, DOI: [10.1021/acs.chemrev.9b00835](https://doi.org/10.1021/acs.chemrev.9b00835).
- 52 R. Nifšler, L. Kurth, H. Li, A. Spreinat, I. Kuhlemann, B. S. Flavel and S. Kruss, Sensing with Chirality-Pure Near-Infrared Fluorescent Carbon Nanotubes, *Anal. Chem.*, 2021, **93**(16), 6446–6455, DOI: [10.1021/acs.analchem.1c00168](https://doi.org/10.1021/acs.analchem.1c00168).
- 53 R. E. Fernandez, Y. Umasankar, P. Manickam, J. C. Nickel, L. R. Iwasaki, B. K. Kawamoto, K. C. Todoki, J. M. Scott and S. Bhansali, Disposable aptamer-sensor aided by magnetic nanoparticle enrichment for detection of salivary cortisol variations in obstructive sleep apnea patients, *Sci. Rep.*, 2017, **7**(7), 17992, DOI: [10.1038/s41598-017-17835-8](https://doi.org/10.1038/s41598-017-17835-8).



- 54 Y. Tanaka, N. A. Binte Mohamed Salleh, M. R. Tan, S. Vij, C. L. Wee, L. Sutarlie and X. Su, A Gold Nanoparticle-Based Cortisol Aptasensor for Non-Invasive Detection of Fish Stress, *Biomolecules*, 2024, **14**(7), 818, DOI: [10.3390/biom14070818](https://doi.org/10.3390/biom14070818).
- 55 J. A. Martin, J. L. Chávez, Y. Chushak, R. R. Chapleau, J. Hagen and N. Kelley-Loughnane, Tunable stringency aptamer selection and gold nanoparticle assay for detection of cortisol, *Anal. Bioanal. Chem.*, 2014, **406**, 4637–4647, DOI: [10.1007/s00216-014-7883-8](https://doi.org/10.1007/s00216-014-7883-8).
- 56 K. G. Butler, Relationship Between the Cortisol-Estradiol Phase Difference and Affect in Women, *J. Circadian Rhythms*, 2018, **16**, 3, DOI: [10.5334/jcr.154](https://doi.org/10.5334/jcr.154).
- 57 P. Gaikwad, N. Rahman, R. Parikh, J. Crespo, Z. Cohen and R. M. Williams, Optical Nanosensor Passivation Enables Highly Sensitive Detection of the Inflammatory Cytokine Interleukin-6, *ACS Appl. Mater. Interfaces*, 2024, **16**(21), 27102–27113, DOI: [10.1021/acsami.4c02711](https://doi.org/10.1021/acsami.4c02711).
- 58 M. Holub, O. Beran, O. Džupová, J. Hnyková, Z. Lacinová, J. Příhodová, B. Procházka and M. Helcl, Cortisol levels in cerebrospinal fluid correlate with severity and bacterial origin of meningitis, *Crit. Care*, 2007, **11**, 1–9, DOI: [10.1186/cc5729](https://doi.org/10.1186/cc5729).
- 59 C. Heidbrink, S. F. Häusler, M. Buttman, M. Ossadnik, H. M. Strik, A. Keller, D. Buck, E. Verbraak, M. van Meurs and M. Krockenberger, Reduced cortisol levels in cerebrospinal fluid and differential distribution of 11 $\beta$ -hydroxysteroid dehydrogenases in multiple sclerosis: implications for lesion pathogenesis, *Brain, Behav., Immun.*, 2010, **24**(6), 975–984, DOI: [10.1016/j.bbi.2010.04.003](https://doi.org/10.1016/j.bbi.2010.04.003).
- 60 J. Popp, S. Wolfsgruber, I. Heuser, O. Peters, M. Hüll, J. Schröder, H.-J. Möller, P. Lewczuk, A. Schneider and H. Jahn, Cerebrospinal fluid cortisol and clinical disease progression in MCI and dementia of Alzheimer's type, *Neurobiol. Aging*, 2015, **36**(2), 601–607, DOI: [10.1016/j.neurobiolaging.2014.10.031](https://doi.org/10.1016/j.neurobiolaging.2014.10.031).
- 61 T. Iqbal, A. Elahi, W. Wijns and A. Shahzad, Cortisol detection methods for stress monitoring in connected health, *Health Sci. Rev.*, 2023, **6**, 100079.
- 62 T. Hianik, V. Ostatná, M. Sonlajtnerova and I. Grman, Influence of ionic strength, pH and aptamer configuration for binding affinity to thrombin, *Bioelectrochemistry*, 2007, **70**(1), 127–133, DOI: [10.1016/j.bioelechem.2006.03.012](https://doi.org/10.1016/j.bioelechem.2006.03.012).
- 63 P.-J. J. Huang, R. Kempaiah and J. Liu, Synergistic pH effect for reversible shuttling aptamer-based biosensors between graphene oxide and target molecules, *J. Mater. Chem.*, 2011, **21**, 8991–8993, DOI: [10.1039/C1JM11702E](https://doi.org/10.1039/C1JM11702E).
- 64 N. Arroyo-Currás, Aptamers Can Be Effective Affinity Receptors for Biosensing, *ECS Sens. Plus*, 2024, **3**(3), 030001.
- 65 M. Belleperche and M. C. DeRosa, pH-control in aptamer-based diagnostics, therapeutics, and analytical applications, *Pharmaceuticals*, 2018, **11**(3), 80, DOI: [10.3390/ph11030080](https://doi.org/10.3390/ph11030080).

